Half-Car 2D Model Simulation of the Self-Adjustable VZN Shock Absorber Suspension Behavior

ADRIAN-IOAN NICULESCU, DAN DUMITRIU, TUDOR SIRETEANU
Institute of Solid Mechanics – Romanian Academy
Str. Constantin Mille, nr. 15, 010141 Bucharest
ROMANIA

Abstract: - The new self-adjustable VZN shock absorber confers improved flexibility to adjust each stroke part according to the specific needs, providing a larger range of damping coefficients, function of the relative piston position in the cylinder. Both on rebound and compression, the VZN damping coefficients have low values at the beginning of the strokes, becoming medium at the middle of the strokes and high and very high to its end. Using a 2D half-car model for vehicle suspension, a Matlab/Simulink simulation was performed in order to compare the VZN with a standard shock absorber. The simulation tests proved better body stability-skyhook comportment, better protection at the stroke ends and lower RMS body accelerations when using the new self-adjustable VZN suspension, all this improvements for almost the same price and the same technological simplicity as a standard suspension.

Key-Words: - self-adjustable VZN, shock absorber, half-car 2D model, Matlab/Simulink, skyhook behavior, comfort, wheel-road adherence, stroke ends protection.

1 Introduction

The proposed self-adjustable shock absorber is called VZN, this acronym coming from Variable Zeta Navigation, where zeta represents the relative damping, which is adjusted automatically, stepwise, according to the piston position. As shown in Fig.1 for the case of compression stroke, the damping fluid flows out the VZN through around 20 metering holes, placed laterally along the inner cylinder.

Thus, for VZN the damping force is adjusted stepwise, as function of the instantaneous piston position, i.e., both on rebound and compression the damping coefficients have: low values at the beginning of the strokes (the hydraulic fluid flows out through all the metering holes); moderate values at the middle of the strokes, for a good tradeoff between comfort and wheel adherence (the hydraulic fluid flows out through half of the metering holes); high values in the working area between middle and end strokes, for better adherence and good axle movement brake (the fluid flows out through quarter of the metering holes); and very high values at the end of the strokes, for better body and axles protection (the fluid flows out through only one or two metering holes).

Realized without electronics or mechanisms, this new VZN concept of shock absorbers has been granted with European Patent EP 1190184 [6] and Romanian Patent 118546 [7]. The design of this passive dynamic VZN shock absorber was so far optimized considering the piston position on full loads and unloads and for end strokes movement high breaking.

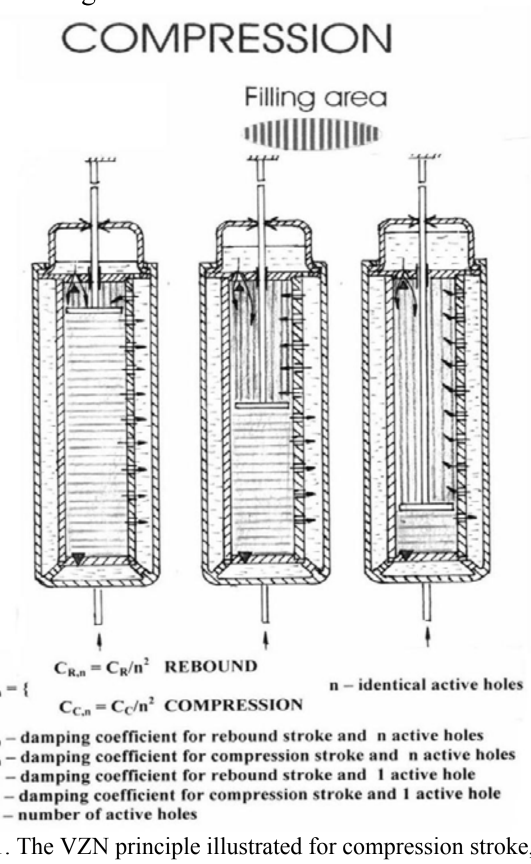

Fig.1. The VZN principle illustrated for compression stroke, with the distributed metering holes placed laterally.

In what concerns the quality/price ratio, the passive dynamic VZN shock absorber realizes an improved and better adapted damping than a standard suspension, for more or less the same price and technological simplicity.

Previous papers [1],[3]-[5] presented the behavior of a suspension using the new self-adjustable VZN shock absorber, simulated on a quarter-car vehicle model. In this paper, the Matlab/Simulink simulation of the VZN behavior is extended from the quarter-car model to the half-car 2D model, in order to better approach the real 3D environment. The simulations performed in this more realistic context confirm the conclusions of the previous quarter-car model simulation, showing improved comfort and adherence performances of the self-adjustable VZN shock absorber, compared with standard shock absorbers. Thus, better body stability-skyhook comportment, better protection at the stroke ends and lower RMS body accelerations were obtained using VZN suspension. Other advantages consist in decreasing lift/squat at acceleration, decreasing dive/lift at braking and decreasing pitch/roll. Ongoing test-bench experiments are performed to prove the advantages of the new self-adjustable VZN shock absorber pointed out by computer simulation.

2 Half-Car 2D Dynamic Model

Fig.2 shows the half-car 2D dynamic model [2],[8]-[9] used to study the vertical interaction between car and road, considering the pitch motion of the car. The model has 4 degrees of freedom, i.e., the vertical displacement x_1 of the front of the car body (front bounce), the vertical displacement x_2 of the back of the car body (rear bounce), the vertical displacement x_3 of the front wheel center (front wheel hop) and the vertical displacement x_4 of the rear wheel center (rear wheel hop). At time t, the vertical profile of the road (road roughness) corresponding to the front wheel is denoted by $x_{01}(t)$ and the road roughness corresponding to the rear wheel is denoted by $x_{02}(t)$. The model contains two levels of elastic and damping elements: one level between the wheels and the road, characterized by the stiffness coefficients k_0' and k_0'' of the tires and the damping coefficients c_0' and c_0'' of the tires; the second level between the wheels and the body (vehicle suspension), characterized by the spring rates of suspension k' and k'' and the damping coefficients c' and c'' of the two VZN shock absorbers (or two standard shock absorbers, as comparison variant).

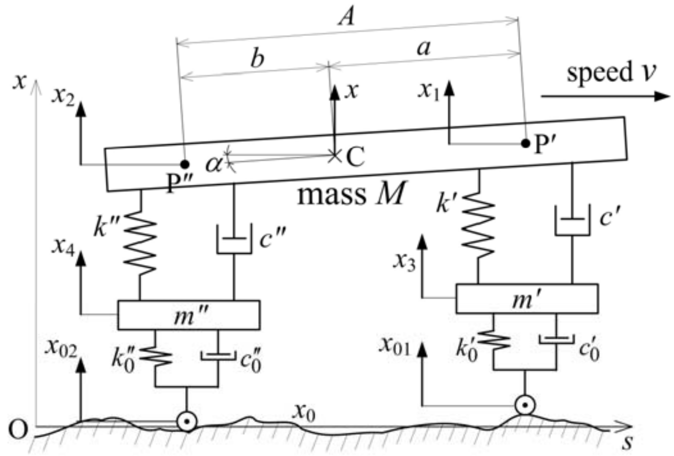

Fig.2. Half-car 2D dynamic model.

The 2D car/road vertical interaction model in Fig.2 implies the following geometrical and inertial characteristics:

- the distance a between the mass center C of the sprung mass M and the point P′ located on the vertical axis passing through the front wheel center;
- the distance b between the mass center C of the sprung mass M and the point P″ located on the vertical axis passing through the rear wheel center;
- the wheel base A of the car (obviously $A=a+b$);
- the front unsprung mass m', i.e., half of the mass of the front wheels and axle;
- the rear unsprung mass m'', i.e., half of the mass of the rear wheels and axle;
- the mass M of the car body (sprung mass M), which normally takes values between M_{empty} (unloaded car case, including only seat+driver and fuel masses) and M_{full} (maximum admissible car loading case);
- the moment of inertia I_α of the sprung mass M with respect to the transversal axis passing through the mass center C of the sprung mass.

2.1 Car body and wheels dynamic equations

The two dynamic equations of the car body, one in terms of forces and the other in terms of moments with respect to the mass center C, are:

$$\begin{cases} \dfrac{Mb}{2A}\ddot{x}_1 + \dfrac{Ma}{2A}\ddot{x}_2 = -F_c' - F_c'' - k'(x_1 - x_3) \\ \qquad - k''(x_2 - x_4) + F'_{e,\text{bumper}} + F''_{e,\text{bumper}} \\ -\dfrac{\rho_\alpha^2 M}{2A}\ddot{x}_1 + \dfrac{\rho_\alpha^2 M}{2A}\ddot{x}_2 = aF_c' - bF_c'' + ak'(x_1 - x_3) \\ \qquad - bk''(x_2 - x_4) - aF'_{e,\text{bumper}} + bF''_{e,\text{bumper}} \end{cases} \tag{1}$$

where F_c' and F_c'' are the damping forces given by the shock absorbers (see expressions (3) and (4)),

$\rho_\alpha = \sqrt{\dfrac{I_\alpha}{M}}$ is the radius of gyration of the sprung mass M with respect to the transversal axis passing through its mass center C; finally $F'_{e,\text{bumber}}$ and $F''_{e,\text{bumber}}$ represent the elastic striking forces when the piston hits either the rebound bumper ($F_{e,\text{bumber}} < 0$ case) or the compression bumper ($F_{e,\text{bumber}} > 0$ case), as detailed in §2.2.

The two dynamic equations of the front and rear wheels are:

$$\begin{cases} m'\ddot{x}_3 = F'_c - c'_0(\dot{x}_3 - \dot{x}_{01}) + k'(x_1 - x_3) \\ \qquad - k'_0(x_3 - x_{01}) - F'_{e,\text{bumper}} \\ m''\ddot{x}_4 = F''_c - c''_0(\dot{x}_4 - \dot{x}_{02}) + k''(x_2 - x_4) \\ \qquad - k''_0(x_4 - x_{02}) - F''_{e,\text{bumper}} \end{cases} \tag{2}$$

The second order differential equations of motion (1) and (2) can be easily transformed in a system of four first order explicit ordinary differential equations, ready to be numerically integrated by usual methods, e.g., the Runge-Kutta method.

For the VZN shock absorber, the damping forces are of the form:

$$F'_{c,\text{VZN}} = c'_{\text{VZN}}(\dot{x}_1 - \dot{x}_3)^2 , \quad F''_{c,\text{VZN}} = c''_{\text{VZN}}(\dot{x}_2 - \dot{x}_4)^2 . \tag{3}$$

The evolution laws of the damping coefficients c'_{VZN} and c''_{VZN} for VZN are so far confidential. c'_{VZN} and c''_{VZN} increase from 0.1 [kN·s/m] up to 350 [kN·s/m] on rebound stroke, and from 0.2 [kN·s/m] up to 600 [kN·s/m] on compression stroke, i.e., more than 3000 times between their minimum and maximum values, depending on the instantaneous piston position.

For the considered standard shock absorber, the damping forces $F'_{c,\text{standard}}$ and $F''_{c,\text{standard}}$ can be approximated as follows:

$$F'_{c,\text{standard}} = \begin{cases} 1.87 \cdot |\dot{x}_1 - \dot{x}_3|^{0.9124} \text{ [kN]}, & \text{if } \dot{x}_1 - \dot{x}_3 \geq 0 \\ -0.6975 \cdot |\dot{x}_1 - \dot{x}_3|^{0.4013} \text{ [kN]}, & \text{if } \dot{x}_1 - \dot{x}_3 \leq 0 \end{cases},$$

$$F''_{c,\text{standard}} = \begin{cases} 1.87 \cdot |\dot{x}_2 - \dot{x}_4|^{0.9124} \text{ [kN]}, & \text{on rebound} \\ -0.6975 \cdot |\dot{x}_2 - \dot{x}_4|^{0.4013} \text{ [kN]}, & \text{on compr.} \end{cases} \tag{4}$$

The road/wheel adherence forces are given by:

$$F'_{\text{adh}} = \begin{cases} -[k'_0(x_3 - x_{01}) + c'_0(\dot{x}_3 - \dot{x}_{01})], & \text{if contact} \\ 0, & \text{if tyre to ground contact lost} \end{cases}$$

$$F''_{\text{adh}} = \begin{cases} -[k''_0(x_4 - x_{02}) + c''_0(\dot{x}_4 - \dot{x}_{02})], & \text{if contact} \\ 0, & \text{if contact lost.} \end{cases}$$

2.2 Kinematic shock absorber model

The kinematic shock absorber model is presented in Fig.3, where $F_{e,\text{bumber}}$ stands for the elastic striking force on stop bumpers.

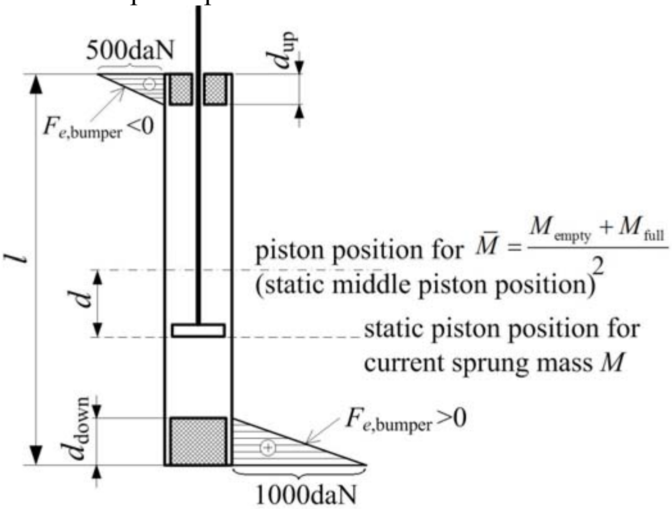

Fig.3. Scheme of the shock absorber.

As shown in Fig.3, $F_{e,\text{bumber}}$ increases linearly from 0 to -500 [daN] beginning at the touch point of rebound bumper, up to the d_{up} distance (stroke of the rebound stop bumper), respectively decreases linearly from 0 to 1000 [daN] beginning at the touch point of the compression bumper, down to d_{down} distance (stroke of the compression stop bumper). Otherwise, $F_{e,\text{bumber}}$ is null. In Fig.3, l is the the full stroke, $l - (d_{\text{up}} + d_{\text{down}})$ the free stroke and d is the distance between the static middle piston position (corresponding to $\bar{M} = \dfrac{M_{\text{empty}} + M_{\text{full}}}{2}$) and the static equilibrium piston position for the current value of the sprung mass M. For the front and respectively rear shock absorbers, this distance d is given by:

$$d' = \left(\bar{M} - M\right)\frac{b}{2A}\frac{g}{k'}, \quad d'' = \left(\bar{M} - M\right)\frac{a}{2A}\frac{g}{k''} .$$

3 Case Study and Results

The considered car has the following geometrical, inertial, elastic and damping characteristics:

- $a = 1.223$ [m], $b = 1.218$ [m], the wheel base $A = a + b = 2.441$ [m];
- the front unsprung mass $m' = 31.5$ [kg],
- the rear unsprung mass $m'' = 30$ [kg],
- the empty and full masses of the car body $M_{\text{empty}} = 0.96$ [t] and $M_{\text{full}} = 1.44$ [t];

- the moment of inertia $I_\alpha = 0.913\ [\mathrm{t \cdot m^2}]$;
- shock absorber dimensions $l = 0.236\ [\mathrm{m}]$, $d_{\mathrm{up}} = 0.014\ [\mathrm{m}]$, $d_{\mathrm{down}} = 0.040\ [\mathrm{m}]$;
- spring rates of suspension $k' = 11.37\ [\mathrm{kN/m}]$ and $k'' = 14.10\ [\mathrm{kN/m}]$;
- stiffness coefficients of the tires $k_0' = 167\ [\mathrm{kN/m}]$ and $k_0'' = 218\ [\mathrm{kN/m}]$,
- tires damping coefficients $c_0' = \dfrac{16.7}{2\pi f}\ [\mathrm{kN \cdot s/m}]$ and $c_0'' = \dfrac{21.8}{2\pi f}\ [\mathrm{kN \cdot s/m}]$, where $f = \max(f_1, f_2, f_3)$ is the maximum frequency among the frequencies of the harmonic functions composing the considered road profile (see §3.1).

The simulations are performed for a car speed of $v = 80\ [\mathrm{km/h}]$.

3.1 Road conditions

In what concerns the road conditions, the best choice is to consider a real road roughness profile or random road profiles with specified spectral density [10]. As in [4], the road profile considered below is simply a sum of three harmonic functions:

$$x_0 = a_1 \sin(2\pi f_1 + \phi_1) + a_2 \sin(2\pi f_2 + \phi_2) + a_3 \sin(2\pi f_3 + \phi_3). \tag{5}$$

The values of the amplitudes, frequencies and phases of the three harmonic functions appearing in the expression (5) considered for the road profile, are given below in Table 1.

Table 1. Amplitudes, frequencies and phases of the excitation harmonic functions considered in (5).

i	Amplitude a_i [m]	Frequency f_i [Hz]	Phase ϕ_i [rad]
1	0.10	1	0
2	0.03	5	5.0815
3	0.01	10	1.2146

3.2 Results

The road/car vertical interaction has been simulated using Matlab/Simulink. The case of using a VZN shock absorber has been compared with the case of using a standard shock absorber. In Figs.4-5 are shown the time evolutions of the front and rear car body vertical accelerations $\ddot{x}_1$ and $\ddot{x}_2$, for a fully weighted car ($M = M_{\mathrm{full}}$) and road profile as in §3.1. The following root mean squares were calculated: $\mathrm{RMS}(\ddot{x}_{1,\mathrm{VZN}}) = 19.14\ [\mathrm{m/s^2}]$ compared with $\mathrm{RMS}(\ddot{x}_{1,\mathrm{standard}}) = 68.7\ [\mathrm{m/s^2}]$ for the front side of the fully weighted car and road profile as in §3.1, respectively $\mathrm{RMS}(\ddot{x}_{2,\mathrm{VZN}}) = 13.45\ [\mathrm{m/s^2}]$ compared with $\mathrm{RMS}(\ddot{x}_{2,\mathrm{standard}}) = 32.4\ [\mathrm{m/s^2}]$ for the rear side of the car. The difference between using VZN and standard shock absorbers is significant (VZN is better), due in part to the elastic striking forces in the stop bumpers, encountered in this case study only for standard shock absorbers, as shown in Figs.6-7.

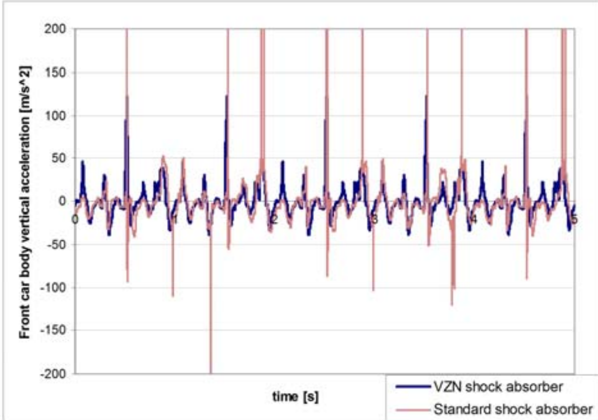

Fig.4. Front car body vertical accelerations $\ddot{x}_1$, for fully weighed car and road profile as in §3.1.

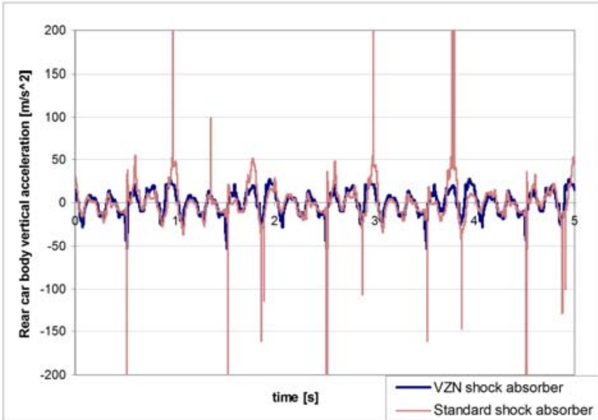

Fig.5. Rear car body vertical accelerations $\ddot{x}_2$, for fully weighed car and road profile as in §3.1.

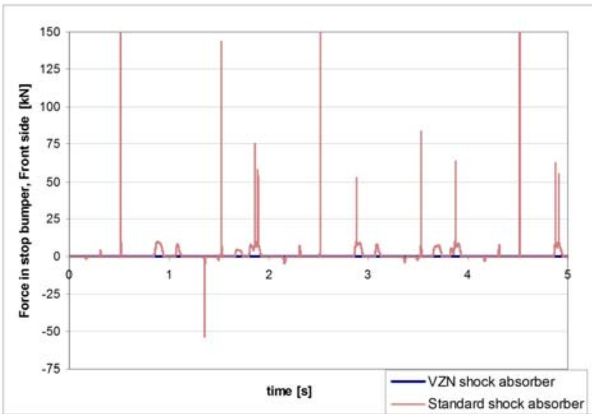

Fig.6. Elastic striking forces in stop bumpers $F'_{e,\mathrm{stop\ bumber}}$, for the front side of a fully weighted car and road profile as in §3.1.

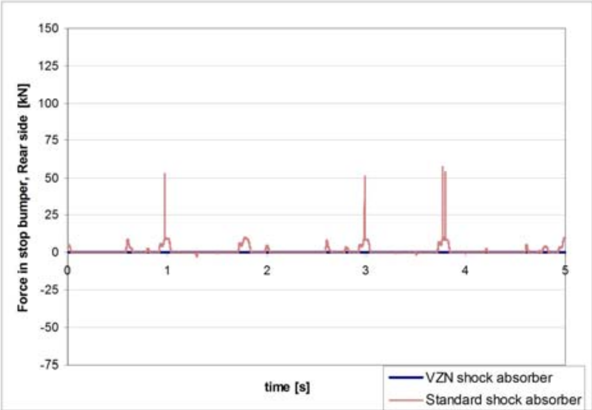

Fig.7. Elastic striking forces in stop bumpers $F''_{e,\text{stop bumber}}$, for the rear side of a fully weighted car and road profile as in §3.1.

Figs.8-9 present the evolutions of the piston strokes, showing less piston motion for the VZN solution. Thus, the standard deviations obtained for the piston strokes are: $\sigma_{x_{13},\text{VZN}} = 4.03$ [cm] compared with $\sigma_{x_{13},\text{standard}} = 6.76$ [cm] for the front side of the fully weighted car and road profile as in §3.1, respectively $\sigma_{x_{24},\text{VZN}} = 4.2$ [cm] compared with $\sigma_{x_{24},\text{standard}} = 5.97$ [cm] for the rear side of the car.

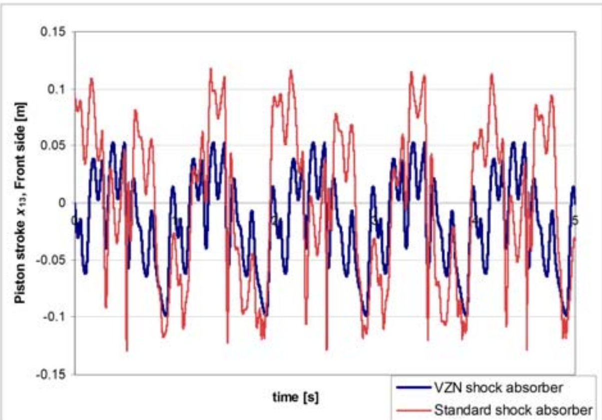

Fig.8. Front piston strokes x_{13}, for fully weighed car and road profile as in §3.1.

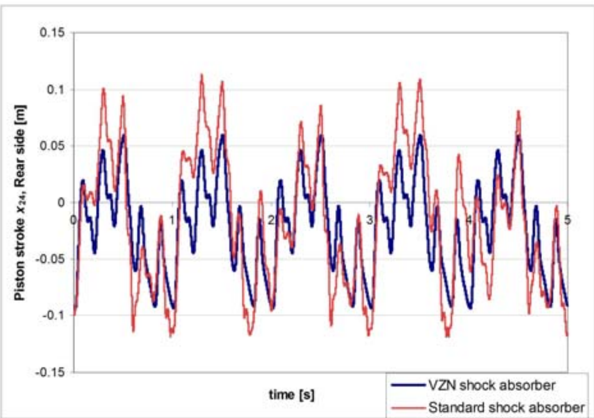

Fig.9. Rear piston strokes x_{24}, for fully weighed car and road profile as in §3.1.

Figs.10-11 show the time evolutions of the front and rear car body vertical displacements x_1 and x_2, for a fully weighted car, as well as the considered road profile (5).

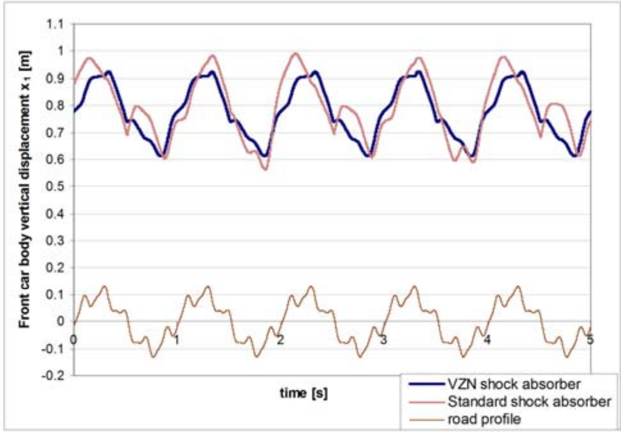

Fig.10. Front bounces x_1 of the car body, for fully weighed car and road profile as in §3.1.

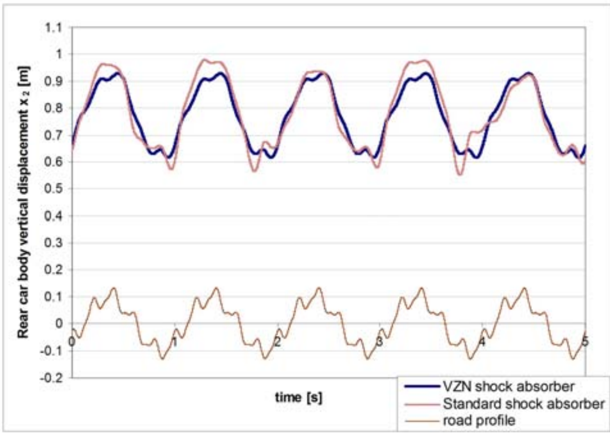

Fig.11. Rear bounces x_2 of the car body, for fully weighed car and road profile as in §3.1.

Finally, the simulation comparison VZN versus standard shock absorber, for a fully loaded car, is performed also for a real Californian road profile, shown in Fig.12.

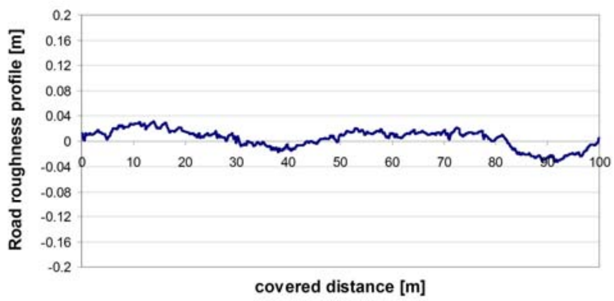

Fig.12. Sample of real Californian road profile.

Figs.13-14 show the time evolutions of the front and rear car body vertical accelerations $\ddot{x}_1$ and $\ddot{x}_2$, for a fully weighted car ($M = M_{\text{full}}$) and the real Californian road profile sample in Fig.12. The following root mean squares were obtained in the case of this real Californian road profile: for the front side $\mathrm{RMS}(\ddot{x}_{1,\mathrm{VZN}}) = 1.09\ [\mathrm{m/s^2}]$ for VZN compared with $\mathrm{RMS}(\ddot{x}_{1,\mathrm{standard}}) = 1.49\ [\mathrm{m/s^2}]$ for standard shock absorber, respectively $\mathrm{RMS}(\ddot{x}_{2,\mathrm{VZN}}) = 1.22\ [\mathrm{m/s^2}]$ compared with $\mathrm{RMS}(\ddot{x}_{2,\mathrm{standard}}) = 1.48\ [\mathrm{m/s^2}]$ for the rear side.

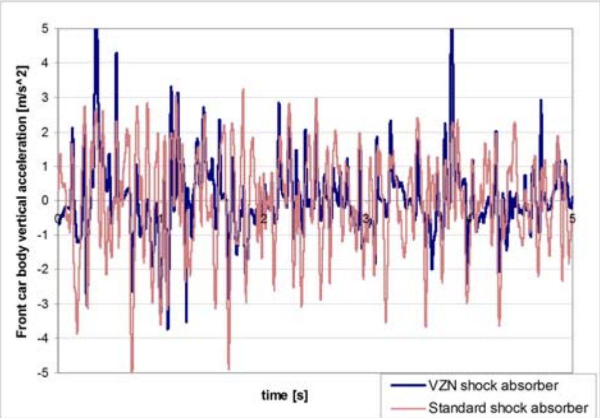

Fig.13. Front car body vertical accelerations $\ddot{x}_1$, for fully weighed car and real Californian road profile.

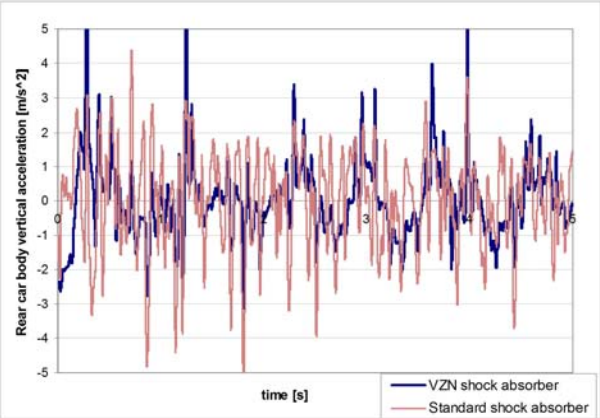

Fig.14. Rear car body vertical accelerations $\ddot{x}_2$, for fully weighed car and real Californian road profile.

4 Conclusion

This paper presents simulation results for a half-car 2D vertical interaction model, in order to test the performances of the new VZN shock absorber. The results obtained so far by simulation show better efficiency of the VZN shock absorber relative to a standard shock absorber, in terms of car body vertical accelerations, skyhook behavior, adherence and axles and body protection at the stroke ends. In fact, for the VZN shock absorber the piston does not hit the stop bumpers, while for the standard shock absorber the piston hits regularly the stop bumpers, with the immediate negative effect on the car body vertical acceleration.

As further work, the VZN shock absorber will be put on a test rig, to verify in practice what have been simulated. Finally, the Simulink code will be used to improve the design of the VZN shock absorber. The purpose is to reach an optimal design, with an optimal behavior of the VZN shock absorber for the considered car and a large variety of road profiles.

References:

[1] A.-I. Niculescu, T. Sireteanu, D. Dumitriu, “Simulation results at some specific regimes, using shock absorbers with primary intelligence - VZN”, *WSEAS European Computing Conference (ECC’07)*, Athens, 25-27 September 2007.

[2] A.-I. Niculescu, „On vehicles axles suspension, collision and rebuff decreasing”, chap.7 in *Research Trends in Mechanics - vol. 1* (eds. D. Popa, V. Chiroiu, I. Toma), Romanian Academy Publishing House, 2007.

[3] A.-I. Niculescu, D. Dumitriu, T. Sireteanu, C. Alexandru, “The new self-adjustable shock absorber VZN”, *31st FISITA World Automotive Congress*, Yokohama, 22-27 October 2006.

[4] A.-I. Niculescu, D. Dumitriu, T. Sireteanu, I. Vieru, “Specific solution for the self adjustable shock absorber VZN”, International Congress Motor Vehicles&Motors, Kragujevac, Serbia, 4-6 October 2006.

[5] A.-I. Niculescu, T. Sireteanu, D. Stăncioiu, “Automotive Self-adjustable Shock Absorber (VZN)”, *30th FISITA World Automotive Congress*, Barcelona, 23-27 May 2004.

[6] A.-I. Niculescu, *Automotive “Self-Adjustable Damper with a Self-Correcting Dissipation Characteristic”*, European Patent EP1190184 / 2005.

[7] A.-I. Niculescu, *Amortizor autocorector, cu caracteristica disipativa autocorectoare*, Romanian Patent 118546/2004.

[8] T. Sireteanu, O. Gündisch, S. Părăian, *Random Vibrations of Automobiles* (in Romanian), Editura Tehnică, Bucharest, 1981.

[9] A.P. Stoicescu, *Dynamics of Automobiles (Stability, Handling and Automotive Vibrations)* (in Romanian), Bucharest Polytechnic Institute Publishing House, 1986.

[10] D. Stăncioiu, T. Sireteanu, M. Giuglea, A.-M. Mitu, “Simulation of Random Road Profiles with Specified Spectral Density”, *Proceedings of the Annual Symposium of the Institute of Solid Mechanics (SISOM’03)*, Bucharest, 15-16 May 2003.